Ikonion Journal of Mathematics 5(2) (2023) 76-91

Ikonion Journal of Mathematics

https://dergipark.org.tr/tr/pub/ikjm

Research Article

Open Access

https://doi.org/10.54286/ikjm.1335660

ISSN: 2687-6531

The Numerical Solutions of the Conformable Time-Fractional Noyes Field Model via a New Hybrid Method

Bedir Kaan ÖNER [1], Halil ANAÇ [2]

Keywords:
Conformable time-fractional Noyes Field model,
q-Sawi homotopy analysis transform method,
Conformable Sawi transform

Abstract — This article employs a novel method, namely the conformable q-Sawi homotopy analysis transform method (Cq-SHATM) to investigate the numerical solutions of the nonlinear conformable time-fractional Noyes-Field model. The proposed method, namely Cq-SHATM, is a hybrid approach that integrates the q-homotopy analysis transform method and the Sawi transform using the concept of conformable derivative. 3D graps of the solutions obtained with this method were drawn. Additionally, 2D graphs of the solutions were obtained in the Maple software program. The computer simulations were conducted in order to validate the efficacy and reliability of the proposed method.

Subject Classification (2020): 65H05,26A33,35R11.

1. Introduction

Beyond the integer order of calculus is the arbitrary order of fractional calculus (FC). When renowned scientists Leibniz and L'Hospital first spoke to one another in roughly 1695, it was discussed. Because fractional calculus may be used to accurately describe a wide variety of nonlinear phenomena, several writers have recently begun to investigate it. Differential equations of the fractional order variety have an impact on both genetic material and non-local material features. Many well-known mathematicians have studied and written on fractional calculus. They created the foundation for fractional calculus through their work. Nowadays, systems that vary over time are frequently studied and nonlinear models created using fractional partial differential equations. Numerous concepts, including chaos theory, have been connected to fractional-order calculus theory. In order to characterize the characteristics of natural systems that don't behave linearly, fractional differential equations are used. We obtain precise answers to fractional differential equations that model nonlinear processes using a variety of analytical and numerical techniques [1–13].

Mohand and Mahgoub [14] introduced a novel integral transform known as the Sawi transform. Problems with population increase and decay were satisfactorily explained using the Sawi transform [15]. In [16], it introduces the "Sawi decomposition method," a novel approach for solving Volterra

[1] onerbedir@outlook.com; [2] halilanac0638@gmail.com (Corresponding Author)
[1] Graduate Education Institute, Gumushane University, Gumushane, Turkey
[2] Torul Vocational School, Gumushane University, Gumushane, Turkey
Article History: Received: 31.07.2023 — Accepted: 24.10.2023 — Published: 20.11.2023

integral equations and its application. The Sawi transformation is employed in the computation of solutions for systems of ordinary differential equations, specifically in the context of determining the concentration of chemical reactants involved in a series chemical reaction [17]. A novel double fuzzy transform, referred to as the double fuzzy Sawi transform, is proposed. This paper presents a formal proof of fundamental properties associated with the single fuzzy Sawi transform and the double fuzzy Sawi transform. The present study employs a technique to derive the precise solution of a non-homogeneous linear fuzzy telegraph equation, incorporating a generalized Hukuhara partial differentiability [18].

The Belousov–Zhabotinsky (B-Z) reaction is a classic example of a chemical oscillating reaction. It was discovered independently by Boris Belousov and Anatol Zhabotinsky in the 1950s. The B-Z reaction is a type of non-equilibrium chemical system that exhibits periodic changes in color, indicating oscillations between different chemical states. One of the remarkable aspects of the B-Z reaction is its ability to exhibit spontaneous oscillations in concentrations of different chemical species. These oscillations are typically observed through changes in color, and the reaction cycles through various states over time. The reaction is autocatalytic, meaning that one of the products of the reaction catalyzes its own formation. This positive feedback loop is essential for the oscillatory behavior observed in the system. The B-Z reaction is relatively complex and involves the interaction of multiple chemical species. It typically includes the oxidation of an organic compound by bromate ions in the presence of various catalysts, such as cerium ions. While the B-Z reaction itself is a fascinating example of chemical kinetics and nonlinear dynamics, its practical applications are limited. However, the principles learned from studying such systems contribute to our understanding of complex dynamic behavior in chemical systems. The Belousov–Zhabotinsky reaction has been of interest in the fields of chemistry and physics, particularly for its ability to illustrate concepts related to chaos and nonlinear dynamics. Researchers have also explored its potential relevance to understanding certain biological processes, as oscillatory behavior is observed in various biological systems. The B-Z reaction is often demonstrated in educational settings to illustrate the dynamic and unpredictable behavior that can arise in chemical systems, challenging the common perception of chemical reactions as static processes.In the current study, we take into consideration the Belousov-Zhabotinsky (B-Z) nonlinear oscillatory system with conformable time-fractional derivative in Caputo sense. The B-Z family of oscillating chemical reactions is intriguing because it can exhibit both spatial traveling concentration waves and temporal oscillations, both of which are accompanied by striking color changes [19]. In a closed system, this reaction can produce up to many thousands of oscillatory cycles, making it possible to study the chemical waves and patterns without having to constantly replace the reactants [20].

For this B-Z, the streamlined conformable time-fractional Noyes-Field model is given as

$$\begin{cases} {}_tT_\mu \rho(x,t) = \vartheta_1 \dfrac{\partial^2 \rho(x,t)}{\partial x^2} + \beta\delta w(x,t) + \rho - \rho^2 - \delta\rho w(x,t), \\ {}_tT_\mu w(x,t) = \vartheta_2 \dfrac{\partial^2 w(x,t)}{\partial x^2} + \gamma w(x,t) - \lambda\rho(x,t) w(x,t). \end{cases} \quad (1)$$

where, ${}_tT_\mu$ is conformable time-fractional oder $\mu \in (0,1]$ in Caputo sense and $0 < t < 1$.

Since the operator in a nonlinear problem with fractional order is described by an integral, these issues are frequently more challenging to solve. The exact and numerical solutions to the fractional problems, however, have been investigated using a variety of computing approaches that have been created. Some of the utilized methods are Adomian decomposition method (ADM) [21-23], variational iteration method (VIM) [24], homotopy analysis method (HAM) [25-28], differential transform method (DTM) [29-30], homotopy perturbation method (HPM) [31-33], residual power series method (RPSM) [34-36], Laplace decomposition method (LDM) [37], q-homotopy analysis method (q-HAM) [38-44], q-homotopy analysis transform method (q-HATM) [45], fractional reduced differential transfofrm method (FRDTM) [45], conformable fractional Elzaki decomposition method (CFEDM) [46], conformable q-homotopy analysis transform method (Cq-HATM) [47], conformable Shehu homotopy perturbation method (CSHPM) [47], conformable fractional q-Shehu homotopy analysis transform method (CFq-SHATM) [48], conformable Shehu transform decomposition method (CSTDM) [48]. The main goal of this study is to come up with a new method: the conformable q-Sawi homotopy analysis transform method (Cq-SHATM).

Here is a list of the rest of the study. The basics of conformable fractional calculus and the Sawi transform are explained in the second part. In Section 3, the new conformable fractional numerical methods are presented. Section 4 shows an example of the conformable time-fractional Noyes Field model. In Section 5, the result is given.

2. Preliminaries

Now let's give the definitions to be used in the study.

Definition 2.1. [49-52] Let a function $f:[0,\infty)\to\mathbb{R}$. Then, the conformable fractional derivative of f order μ is described by

$$T_\mu(f)(x)=\lim_{\varepsilon\to 0}\frac{f(x+\varepsilon x^{1-\mu})-f(x)}{\varepsilon}, \tag{2}$$

for all $x>0, \mu\in(0,1]$.

Theorem 2.1. [49-50, 52] Let $\mu\in(0,1]$ and f,g be μ −differentiable at a point $x>0$. Then

$(i)\ T_\mu(af+bg)=aT_\mu(f)+bT_\mu(g)$, for all $a,b\in\ \mathbb{R}$, (3)

$(ii)\ T_\mu(x^p)=px^{p-1}$, for all $p\in\mathbb{R}$, (4)

$(iii)\ T_\mu(\tau)=0, for\ all\ constant\ functions, f(t)=\tau,$ (5)

$(iv)\ T_\mu(fg)=fT_\mu(g)+gT_\mu(f),$ (6)

$(v)\ T_\mu\left(\frac{f}{g}\right)=\frac{gT_\mu(f)-fT_\mu(g)}{g^2}.$ (7)

Definition 2.2. Let $0<\mu\leq 1$, $f:[0,\infty)\to\mathbb{R}$ be real valued function. Then, the conformable fractional Sawi transform (CFST) of order μ of f is defined by

$$ {}_cS_\mu[f(t)](v) = R_\mu(v) = \frac{1}{v^2}\int_0^\infty exp\left(\frac{-t^\mu}{v\mu}\right) f(t)t^{\mu-1}dt\,, v > 0. \tag{8} $$

Definition 2.3. Let $0 < \mu \leq 1$, $f: [0,\infty) \to \mathbb{R}$ be real valued function. The conformable fractional Sawi transform for the conformable fractional-order derivative of the function $f \in \mathbb{C}_\eta(\eta \geq -1)$ is defined by

$$ {}_cS_\mu\big[T_\mu f(t)\big](v) = \frac{1}{v^\mu} R_\mu(v) - \sum_{k=0}^{\sigma-1}\left(\frac{1}{v}\right)^{\mu-(k-1)} f^{(k)}(0^+), \sigma - 1 < \mu \leq \sigma. \tag{9} $$

3. Conformable q-Sawi Homotopy Analysis Transform Method

We will introduce a new method. Consider the conformable time-fractional nonlinear partial differential equation (CTFNPDE) to explain the fundamental idea of Cq-SHATM:

$$ {}_tT_\mu w(x,t) + Aw(x,t) + Hw(x,t) = f(x,t), n - 1 < \mu \leq n, \tag{10} $$

where A is a linear operator, H is a nonlinear operator, $f(x,t)$ is a source term, and ${}_tT_\mu$ is a conformable time-fractional derivative of order μ.

Applying the conformable fractional Sawi transform to Eq. (10) and utilizing the initial condition, then we have

$$ \frac{{}_cS_\mu[w(x,t)]}{v^\mu} - \sum_{k=0}^{m-1}\left(\frac{1}{v}\right)^{\mu-(k-1)} w^{(k)}(x,0) = {}_cS_\mu[f(x,t) - Aw(x,t) - Hw(x,t)]. \tag{11} $$

Rearranging the last equation, then we get

$$ \begin{aligned} {}_cS_\mu[w(x,t)] - v^\mu \sum_{k=0}^{m-1}\left(\frac{1}{v}\right)^{\mu-(k-1)} w^{(k)}(x,0) + v^\mu\ {}_cS_\mu[Aw(x,t) + Hw(x,t)] \\ - v^\mu\ {}_cS_\mu[f(x,t)] = 0. \end{aligned} \tag{12} $$

With the help of HAM, we can describe the nonlinear operator for real function $\varphi(x,t;q)$ as follows:

$$ N[\varphi(x,t;q)] = {}_cS_\mu[\varphi(x,t;q)] - v^\mu \sum_{k=0}^{m-1}\left(\frac{1}{v}\right)^{\mu-(k-1)} \varphi^{(k)}(x,t;q)(0^+) + v^\mu\ {}_cS_\mu[A\varphi(x,t;q) $$

$$ +H\varphi(x,t;q)] - v^\mu\ {}_cM_\alpha[f(x,t)], \tag{13} $$

where $q\epsilon\left[0,\frac{1}{n}\right]$.

We construct a homotopy as follows:

$$(1-nq)\ {}_{c}S_{\alpha}[\varphi(x,t;q)-w_0(x,t)] = hqH^*(x,t)H[\varphi(x,t;q)], \tag{14}$$

where, $h \neq 0$ is an auxiliary parameter and ${}_{c}S_{\alpha}$ represents conformable fractional Sawi transform. For $q=0$ and $q=\frac{1}{n}$, the results of Eq. (14) are as follows:

$$\varphi(x,t;0) = w_0(x,t), \varphi\left(x,t;\frac{1}{n}\right) = w(x,t). \tag{15}$$

Thus, by amplifying q from 0 to $\frac{1}{n}$, then the solution $\varphi(x,t;q)$ converges from $w_0(x,t)$ to the solution $w(x,t)$.

Using the Taylor theorem around q and then expanding $\varphi(x,t;q)$, we get

$$\varphi(x,t;q) = w_0(x,t) + \sum_{i=1}^{\infty} w_m(x,t)q^m, \tag{16}$$

where

$$w_m(x,t) = \frac{1}{m!}\frac{\partial^m \varphi(x,t;q)}{\partial q^m}|_{q=0}. \tag{17}$$

Eq. (16) converges at $q=\frac{1}{n}$ for the appropriate $w_0(x,t)$, n and h. Then, we have

$$w(x,t) = w_0(x,t) + \sum_{m=1}^{\infty} w_m(x,t)\left(\frac{1}{n}\right)^m. \tag{18}$$

If we differentiate the zeroth order deformation Eq. (14) m-times with respect to q and we divide by $m!$, respectively, then for $q=0$, we acquire

$${}_{c}S_{\alpha}[w_m(x,t) - k_m w_{m-1}(x,t)] = hH^*(x,t)\mathcal{R}_m(\vec{w}_{m-1}), \tag{19}$$

where the vectors are described by

$$\vec{w}_m = \{w_0(x,t), w_1(x,t), \dots, w_m(x,t)\}. \tag{20}$$

Applying the inverse conformable fractional Sawi transform to Eq. (20), we get

$$w_m(x,t) = k_m w_{m-1}(x,t) + h\left({}_{c}S_{\alpha}\right)^{-1}[H^*(x,t)\mathcal{R}_m(\vec{w}_{m-1})], \tag{21}$$

where

$$\mathcal{R}_m(\vec{w}_{m-1}) = {}_{c}S_{\alpha}[w_{m-1}(x,t)] - \left(1-\frac{k_m}{n}\right)\frac{1}{v}w_0(x,t) + v^{\mu}\ {}_{c}S_{\mu}[Aw_{m-1}(x,t)$$

$$+H_{m-1}(x,t) - f(x,t)], \tag{22}$$

and

$$k_m = \begin{cases} 0, & m \leq 1, \\ n, & m > 1. \end{cases} \tag{23}$$

Here, H_m^* is homotopy polynomial and presented by

$$H_m^* = \frac{1}{m!}\frac{\partial^m \varphi(x,t;q)}{\partial q^m}|_{q=0} \text{ and } \varphi(x,t;q) = \varphi_0 + q\varphi_1 + q^2\varphi_2 + \cdots. \tag{24}$$

Using Eqs. (21) - (22), we get

$$\begin{aligned} w_m(x,t) = (k_m + h)w_{m-1}(x,t) - \left(1 - \frac{k_m}{n}\right) w_0(x,t) \\ + \mathrm{h}\left({}_cS_\alpha\right)^{-1}\left[v^\mu \ {}_cS_\mu[Aw_{m-1}(x,t) + H_{m-1}(x,t) - f(x,t)]\right]. \end{aligned} \tag{25}$$

When Cq-SHATM is utilized, the series solution is given by

$$w(x,t) = \sum_{m=0}^{\infty} w_m(x,t)\left(\frac{1}{n}\right)^m. \tag{26}$$

4. Applications

Example 4.1. [45] Consider the conformable time-fractional Noyes Field model

$$\begin{cases} \dfrac{\partial^\mu \rho(x,t)}{\partial t^\mu} = \dfrac{\partial^2 \rho(x,t)}{\partial x^2} + \rho - \rho^2 - \delta\rho w(x,t), \\ \dfrac{\partial^\mu w(x,t)}{\partial t^\mu} = \dfrac{\partial^2 w(x,t)}{\partial x^2} - \lambda\rho w(x,t), \end{cases} \tag{27}$$

where $\lambda \neq 1$ and δ are positive constants, $x \in [-10,10], t \in [0,1], 0 < \mu \leq 1$, subject to initial conditions

$$\begin{cases} \rho(x,0) = \dfrac{1}{\left(\exp\left(\sqrt{\frac{\lambda}{6}}x\right)+1\right)^2}, \\ w(x,0) = \dfrac{(1-\lambda)\exp\left(\sqrt{\frac{\lambda}{6}}x\right)\left(\exp\left(\sqrt{\frac{\lambda}{6}}x\right)+1\right)}{\delta\left(\exp\left(\sqrt{\frac{\lambda}{6}}x\right)+1\right)^2}. \end{cases} \tag{28}$$

Cq-SHATM solution

Implementing the conformable fractional Sawi transform to Eqs. (27) and using Eqs. (28), then it is obtained as

$$\frac{{}_cS_\mu[\rho(x,t)]}{v} - \frac{\rho(x,0)}{v^2} = {}_cS_\mu\left[\frac{\partial^2 \rho(x,t)}{\partial x^2} + \rho - \rho^2 - \delta\rho w(x,t)\right], \tag{29}$$

$$\frac{{}_cS_\mu[w(x,t)]}{v} - \frac{w(x,0)}{v^2} = {}_cS_\mu\left[\frac{\partial^2 w(x,t)}{\partial x^2} - \lambda\rho w(x,t)\right]. \quad (30)$$

Rearranging Eqs.(29)-(30), then we have

$${}_cS_\mu[\rho(x,t)] = \frac{\rho(x,0)}{v} + v\ {}_cS_\mu\left[\frac{\partial^2\rho(x,t)}{\partial x^2} + \rho - \rho^2 - \delta\rho w(x,t)\right], \quad (31)$$

$${}_cS_\mu[w(x,t)] = \frac{w(x,0)}{v} + v\ {}_cS_\mu\left[\frac{\partial^2 w(x,t)}{\partial x^2} - \lambda\rho(x,t)w(x,t)\right]. \quad (32)$$

We define the nonlinear operators by using Eqs. (31)-(32), as

$$N^1[\varphi(x,t;q)\,] = {}_cS_\mu[\varphi(x,t;q)\,] - \frac{1}{v\left(\exp\left(\sqrt{\frac{\lambda}{6}}x\right)+1\right)^2}$$

$$+v\ {}_cS_\mu\left[\frac{\partial^2\varphi(x,t;q)}{\partial x^2} + \varphi(x,t;q) - \varphi^2(x,t;q) - \delta\varphi(x,t;q)\psi(x,t;q)\right], \quad (33)$$

$$N^2[\psi(x,t;q)\,] = {}_cS_\mu[\psi(x,t;q)\,] - \frac{(1-\lambda)\exp\left(\sqrt{\frac{\lambda}{6}}x\right)\left(\exp\left(\sqrt{\frac{\lambda}{6}}x\right)+1\right)}{\delta v\left(\exp\left(\sqrt{\frac{\lambda}{6}}x\right)+1\right)^2}$$

$$+v\ {}_cS_\mu\left[\frac{\partial^2\psi(x,t;q)}{\partial x^2} - \lambda\varphi(x,t;q)\psi(x,t;q)\right]. \quad (34)$$

By applying the proposed algorithm, the $m-th$ order deformation equations are defined by

$${}_cS_\mu[\rho_m(x,t) - k_m\rho_{m-1}(x,t)] = h\mathcal{R}_{1,m}[\vec{\rho}_{m-1}], \quad (35)$$

$${}_cS_\mu[w_m(x,t) - k_m w_{m-1}(x,t)] = h\mathcal{R}_{2,m}[\vec{w}_{m-1}], \quad (36)$$

where

$$\mathcal{R}_{1,m}[\vec{\rho}_{m-1}] = {}_cS_\mu[\vec{\rho}_{m-1}(x,t)] - \left(1-\frac{k_m}{n}\right)\frac{1}{v\left(\exp\left(\sqrt{\frac{\lambda}{6}}x\right)+1\right)^2}$$

$$-v\ {}_cS_\mu\left[\frac{\partial^2\rho_{m-1}(x,t)}{\partial x^2} + \rho_{m-1}(x,t) - \sum_{r=0}^{m-1}\rho_r(x,t)\rho_{m-1-r}(x,t) - \delta\sum_{r=0}^{m-1}\rho_r(x,t)w_{m-1-r}(x,t)\right], \quad (37)$$

$$\mathcal{R}_{2,m}[\vec{w}_{m-1}] = {}_{c}S_{\mu}[\vec{w}_{m-1}(x,t)] - \left(1-\frac{k_m}{n}\right)\frac{(1-\lambda)\exp\left(\sqrt{\frac{\lambda}{6}}x\right)\left(\exp\left(\sqrt{\frac{\lambda}{6}}x\right)+1\right)}{\delta v\left(\exp\left(\sqrt{\frac{\lambda}{6}}x\right)+1\right)^2}$$

$$-v\ {}_{c}S_{\mu}\left[\frac{\partial^2 w_{m-1}(x,t)}{\partial x^2} - \lambda\sum_{r=0}^{m-1}\rho_r(x,t)w_{m-1-r}(x,t)\right]. \quad (38)$$

On applying inverse conformable Sawi transform to Eqs. (35)-(36), then we have

$$\rho_m(x,t) = k_m\rho_{m-1}(x,t) + h\left({}_{c}S_{\mu}\right)^{-1}\{\mathcal{R}_{1,m}[\vec{p}_{m-1}]\}, \quad (39)$$

$$w_m(x,t) = k_m w_{m-1}(x,t) + h\left({}_{c}S_{\mu}\right)^{-1}\{\mathcal{R}_{2,m}[\vec{w}_{m-1}]\}. \quad (40)$$

By the use of initial conditions, then we obtain

$$\rho_0(x,t) = \frac{1}{\left(\exp\left(\sqrt{\frac{\lambda}{6}}x\right)+1\right)^2}, \quad (41)$$

$$w_0(x,t) = \frac{(1-\lambda)\exp\left(\sqrt{\frac{\lambda}{6}}x\right)\left(\exp\left(\sqrt{\frac{\lambda}{6}}x\right)+2\right)}{\delta\left(\exp\left(\sqrt{\frac{\lambda}{6}}x\right)+1\right)^2}. \quad (42)$$

To find the values of $\rho_1(x,t)$ and $w_1(x,t)$, putting $m = 1$ in Eqs. (39)-(40), then we obtain

$$\rho_1(x,t) = -\frac{2}{3}h\frac{t^{\mu}\exp\left(\frac{x\sqrt{6\lambda}}{6}\right)\left(\left(\left(\left(\frac{3}{2}+\lambda\right)\delta+\frac{3}{2}\lambda-\frac{3}{2}\right)\exp\left(\frac{x\sqrt{6\lambda}}{6}\right)+\left(-\frac{\lambda}{2}+3\right)\delta+3\lambda-3\right)}{\mu\delta\left(\exp\left(\frac{x\sqrt{6\lambda}}{6}\right)+1\right)^4}, \quad (43)$$

$$w_1(x,t) = \frac{5}{3}\frac{t^{\mu}(-1+\lambda)\lambda\exp\left(\frac{x\sqrt{6\lambda}}{6}\right)}{\mu\delta\left(\exp\left(\sqrt{\frac{\lambda}{6}}x\right)+1\right)^3}. \quad (44)$$

In the same way, if we put $m = 2$ in Eqs. (39)-(40), we can obtain the values of $\rho_2(x,t)$ and $w_2(x,t)$

$$w_2(x,t)=\frac{-5h(n+h)t^{\mu}(-1+\lambda)\lambda\exp\left(\frac{x\sqrt{6\lambda}}{6}\right)}{3\mu\delta\left(\exp\left(\sqrt{\frac{\lambda}{6}}x\right)+1\right)^3}+\frac{8}{9\mu^2\delta^2\left(\exp\left(\sqrt{\frac{\lambda}{6}}x\right)+1\right)^6}$$

$$\times\left[h^2t^{2\mu}\lambda(-1+\lambda)\exp\left(\frac{x\sqrt{6\lambda}}{6}\right)\left(\frac{-9}{4}(-1+\lambda)(\delta-1)\exp\left(\frac{x\sqrt{6\lambda}}{6}\right)+\left(\left(\delta+\frac{9}{16}\right)\lambda+\frac{9}{16}\delta\right.\right.\right.$$

$$\left.\left.\left.-\frac{9}{16}\right)\exp\left(\frac{x\sqrt{6\lambda}}{6}\right)+\frac{3}{4}\left(-3+(3+\frac{\delta}{8}\right)\lambda+3\delta)\exp\left(\frac{x\sqrt{6\lambda}}{6}\right)-\frac{25}{32}\lambda\delta\right)\right]. \tag{46}$$

In this way, the other terms can be found. So, the Cq-SHATM solutions of the Eq. (27) are given by

$$\rho(x,t)=\rho_0(x,t)+\sum_{m=1}^{\infty}\rho_m(x,t)\left(\frac{1}{n}\right)^m, \tag{47}$$

$$w(x,t)=w_0(x,t)+\sum_{m=1}^{\infty}w_m(x,t)\left(\frac{1}{n}\right)^m. \tag{48}$$

If we put $\mu=1, n=1,\ h=-1$ in Eqs. (47)-(48), then the obtained results

$$\sum_{m=1}^{M}\rho_m(x,t)\left(\frac{1}{n}\right)^m, \sum_{m=1}^{M}w_m(x,t)\left(\frac{1}{n}\right)^m$$

converges to the exact solutions

$$\rho(x,t)=\frac{\exp\left(\frac{5\lambda}{3}t\right)}{\left(\exp\left(\sqrt{\frac{\lambda}{6}}x\right)+\exp\left(\frac{5\lambda}{6}t\right)\right)^2}\ w(x,t)=\frac{(1-\lambda)\exp\left(\sqrt{\frac{\lambda}{6}}x\right)\left(\exp\left(\sqrt{\frac{\lambda}{6}}x\right)+2\exp\left(\frac{5\lambda}{6}t\right)\right)}{\delta\left(\exp\left(\sqrt{\frac{\lambda}{6}}x\right)+\exp\left(\frac{5\lambda}{6}t\right)\right)^2}$$

of the Eqs. (27) when $M\to\infty$.

Figure 1 shows the 3D graphs of $\rho(x,t)$ solution for Cq-SHATM, $w(x,t)$solution for Cq-SHATM, exact solutions of $\rho(x,t)$, $w(x,t)$ and absolute errors.

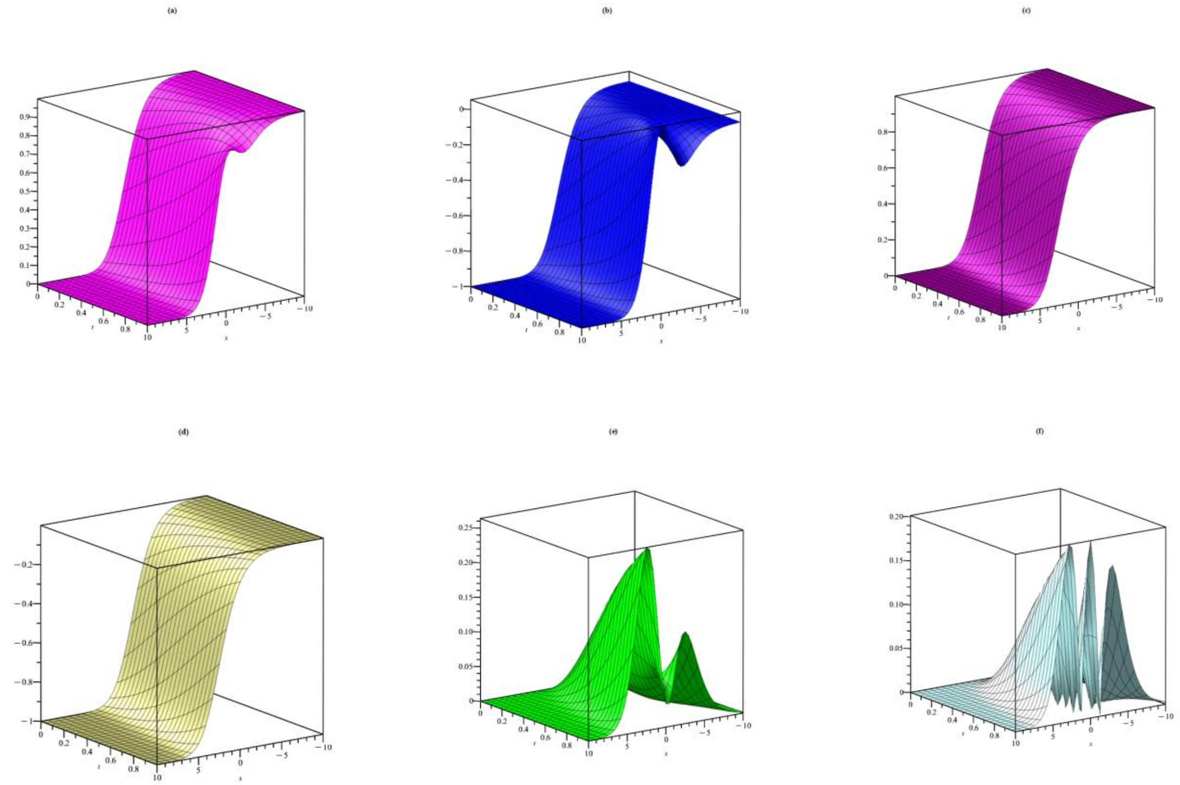

Figure 1. (a) Nature of $\rho(x,t)$solution with Cq-SHATM **(b)** Nature of $w(x,t)$solution with Cq-SHATM **(c)** Exact of $\rho(x,t)$ solution **(d)** Exact of $w(x,t)$ solution **(e)** Nature of absolute error=$|\rho_{exact}-\rho_{Cq-SHATM}|$ **(f)** Nature of absolute error=$|w_{exact}-w_{Cq-SHATM}|$ at $h=-1, n=1, \mu=1, \lambda=3, \delta=2$ for Eqs. (37).

Figure 2 depicts comparison 2D plots of $\rho(x,t)$ solution with Cq-SHATM, $w(x,t)$ solution with Cq-SHATM, and exact solutions for distinct μ values.

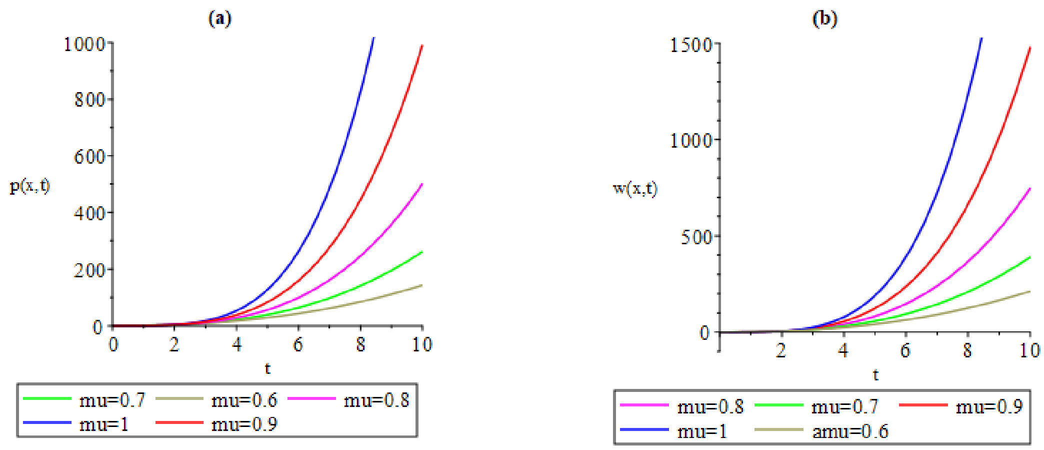

Figure 2. The comparison of the $\rho(x,t)$ solution with Cq-SHATM and exact solution **(b)** The comparison of the $w(x,t)$ solution with Cq-SHATM and exact solution at $h=-1, n=1, x=0.5, \lambda=3, \delta=2$ with different μ for Eqs. (37).

A comparison of the absolute error for $\rho(x,t)$ between Cq-SHATM and FRDTM [45] for Eq. (37) with $\mu = 1, \lambda = 3, \delta = 2, h = -1, n = 1$ is presented in Table 1.

x		**t**			
		0.001	**0.003**	**0.005**	**0.007**
Cq-SHATM	**0.00**	0.0001878902	0.0005660070	0.0009472246	0.0013315278
FRDTM		1.0149996100	1.0137464930	1.0124902750	1.0112309720
Cq-SHATM	**1.00**	0.0000976247	0.0002956422	0.0004973550	0.0007027695
FRDTM		0.8256007700	0.8248666560	0.8241288453	0.8233873339
Cq-SHATM	**2.00**	0.0000370568	0.0001128071	0.0001907491	0.0002708944
FRDTM		0.4254561817	0.4251463250	0.4248342767	0.4245200242
Cq-SHATM	**3.00**	0.0000114341	0.0000349498	0.0000593341	0.0000845935
FRDTM		0.1584645226	0.1583613457	0.1582572998	0.1581523788

Table 1. Comparison of absolute error for $\rho(x,t)$ between Cq-SHATM and FRDTM [45] for Eq. (37) with $\mu = 1, \lambda = 3, \delta = 2, h = -1, n = 1$.

Comparing the absolute errors for $w(x,t)$ for Eq. (37) with $\mu = 1, \lambda = 3, \delta = 2, h = -1, n = 1$ for Cq-SHATM and FRDTM [45] is provided in Table 2.

x		**t**			
		0.001	**0.003**	**0.005**	**0.07**
Cq-SHATM	**0.00**	3.9×10^{-7}	3.5×10^{-6}	9.7×10^{-6}	1.9×10^{-5}
FRDTM		1.0149996100	1.0137464930	1.0124902750	1.0112309720
Cq-SHATM	**1.00**	4.6×10^{-7}	4.1×10^{-6}	0.0000115353	0.0000226217
FRDTM		0.8256007696	0.8248666555	0.8241288453	0.8233873341
Cq-SHATM	**2.00**	2.7×10^{-7}	2.4×10^{-6}	6.8×10^{-6}	0.0000134002
FRDTM		0.4254561817	0.4251463250	0.4248342767	0.4245200246
Cq-SHATM	**3.00**	1.0×10^{-7}	9.6×10^{-7}	2.7×10^{-6}	5.3×10^{-6}
FRDTM		0.1584645226	0.1583613454	0.1582572998	0.1581523789

Table 2. Comparison of absolute error for $w(x,t)$ between Cq-SHATM and FRDTM [45] for Eq. (37) with $\mu = 1, \lambda = 3, \delta = 2, h = -1, n = 1$.

5. Conclusion (if necessary)

Figure 1 displays the three-dimensional graphs of the Cq-SHATM solutions $\rho(x,t)$ and $w(x,t)$, the exact solutions of $\rho(x,t)$ and $w(x,t)$, as well as the absolute errors for Eq. (27). Figure 2 illustrates a comparison of two-dimensional plots of the solutions $\rho(x,t)$ and $w(x,t)$ obtained using the Cq-SHATM, as well as the corresponding exact solutions for different values of μ. Table 1 presents a comparison of the absolute error for the function $\rho(x,t)$ between the Cq-SHATM and FRDTM methods [45] for Eq. (27), with the parameter values $\mu = 1, \lambda = 3, \delta = 2, h = -1$, and $n = 1$. Table 2 presents a comparison of the absolute errors of $w(x,t)$ for Eq. (27) with the given parameter values $\mu = 1, \lambda = 3, \delta = 2, h = -1$, and $n = 1$, between Cq-SHATM and FRDTM in [45]. The data presented in Tables 1-2 indicates that the Cq-SHATM exhibits a significantly lower error rate in comparison to the FRDTM in [45]. The results presented in Tables 1-2 demonstrate that the techniques proposed in this study yield significantly superior outcomes compared to those achieved through the utilization of FRDTM.

The present study aims to examine the behavior of conformable time-fractional Noyes Field model through the utilization of Cq-SHATM. In addition, the utilization of the MAPLE software has been employed to generate two-dimensional and three-dimensional graphs that illustrate the solutions to Eq. (37) for various values of $\mu = 1$. Observations have been made regarding the variations in the overall structure of the surface graphs produced by the Maple computational software for Eq. (37). Differences in the overall configuration of surface graphs generated by the Maple software for Eq. (37) have been observed. The study findings indicated that the approaches presented in Tables 1-2 produced results that are much better than those obtained through the use of FRDTM, with the independent variable being t and x being held at a constant value. A new hybrid method is proposed. This method is Cq-SHATM, which is a combination of the conformable Sawi transform and the q-homotopy analysis transform method. With this new method, new numerical solutions of the conformable Noyes-Field model have been obtained. It has been observed that this solution provides better results than the FRDTM existing in the literature. The effectiveness and advantages of the recently developed method for tackling nonlinear conformable time-fractional models have been acknowledged. The recent method proposed for the resolution of nonlinear conformable time-fractional models have been determined to possess distinct advantages and demonstrate notable efficacy.

Author Contributions

All authors contributed equally to this work. They all read and approved the final version of the manuscript.

Conflicts of Interest

The authors declare no conflict of interest.

References

[1] Miller, K. S., Ross, B. 1993. An introduction to the fractional calculus and fractional differential equations, Wiley, New York, 376 p.

[2] Podlubny, I. 1999. Fractional differential equations, mathematics in science and engineering, Academic Press, New York, 365 p.

[3] Baleanu, D., Diethelm, K., Scalas, E., Trujillo, J. J. 2012. *Fractional calculus: models and numerical methods*, World Scientific, London, 476 p.

[4] Povstenko, Y. 2015. Linear fractional diffusion-wave equation for scientists and engineers. Birkhäuser, Switzerland, 460 p.

[5] Ala, V. 2022. New exact solutions of space-time fractional Schrödinger-Hirota equation. Bulletin of the Karaganda university Mathematics series, 107(3), 17-24.

[6] Ala, V. 2023. Exact Solutions of Nonlinear Time Fractional Schrödinger Equation with Beta- Derivative. Fundamentals of Contemporary Mathematical Sciences, 4(1), 1-8.

[7] Baleanu, D., Wu, G. C., Zeng, S. D. 2017. Chaos analysis and asymptotic stability of generalized Caputo fractional differential equations. Chaos, Solitons & Fractals, 102, 99-105.

[8] Sweilam, N. H., Abou Hasan, M. M., Baleanu, D. 2017. New studies for general fractional financial models of awareness and trial advertising decisions. Chaos, Solitons & Fractals, 104, 772-784.

[9] Liu, D. Y., Gibaru, O., Perruquetti, W., Laleg-Kirati, T. M. 2015. Fractional order differentiation by integration and error analysis in noisy environment. *IEEE Transactions on Automatic Control*, *60(11)*, 2945-2960.

[10] Esen, A., Sulaiman, T. A., Bulut, H., Baskonus, H. M. 2018. Optical solitons to the space-time fractional (1+1)-dimensional coupled nonlinear Schrödinger equation. Optik, 167, 150-156.

[11] Veeresha, P., Prakasha, D. G., Baskonus, H. M. 2019. Novel simulations to the time-fractional Fisher's equation. Mathematical Sciences, 13(1), 33-42.

[12] Veeresha, P., Prakasha, D. G., Baskonus, H. M. 2019. New numerical surfaces to the mathematical model of cancer chemotherapy effect in Caputo fractional derivatives. Chaos: An Interdisciplinary Journal of Nonlinear Science, 29(1), 013119. https://doi.org/10.1063/1.5074099.

[13] Caponetto, R., Dongola, G., Fortuna, L., Gallo, A. 2010. New results on the synthesis of FO-PID controllers. Communications in Nonlinear Science and Numerical Simulation, 15(4), 997-1007.

[14] Mahgoub, M. A., & Mohand, M. (2019). The new integral transform "Sawi Transform". Advances in Theoretical and Applied Mathematics, 14(1), 81-87.

[15] Singh, G. P., & Aggarwal, S. (2019). Sawi transform for population growth and decay problems. *International Journal of Latest Technology in Engineering, Management & Applied Science*, *8*(8), 157-162.

[16] Higazy, M., Aggarwal, S., & Nofal, T. A. (2020). Sawi decomposition method for Volterra integral equation with application. *Journal of Mathematics*, *2020*, 1-13.

[17] Higazy, M., Aggarwal, S. (2021). Sawi transformation for system of ordinary differential equations with application. *Ain Shams Engineering Journal*, *12*(3), 3173-3182.

[18] Georgieva, A. T., & Pavlova, A. (2023). Application of the Double Fuzzy Sawi Transform for Solving a Telegraph Equation. *Symmetry*, *15*(4), 854.

[19] Gibbs, R. G. (1980). Traveling waves in the Belousov–Zhabotinskii reaction. *SIAM Journal on Applied Mathematics*, *38*(3), 422-444.

[20] Zhabotinsky Anatol M (2007) Scholarpedia 2(9):1435. https://doi.org/10.4249/scholarpedia

[21] Ray, S. S., & Bera, R. K. (2006). Analytical solution of a fractional diffusion equation by Adomian decomposition method. *Applied Mathematics and Computation*, *174*(1), 329-336.

[22] Adomian, G. (1994). Solving frontier problems of physics: the decomposition method, Springer. *Dordrecht*.

[23] Wazwaz, A. M., & Gorguis, A. (2004). An analytic study of Fisher's equation by using Adomian decomposition method. *Applied Mathematics and Computation*, *154*(3), 609-620.

[24] Das, S. (2009). Analytical solution of a fractional diffusion equation by variational iteration method. *Computers & Mathematics with Applications*, *57*(3), 483-487.

[25] Liao, S. J. (1995). An approximate solution technique not depending on small parameters: a special example. *International Journal of Non-Linear Mechanics*, *30*(3), 371-380.

[26] Shijun, L. (1998). Homotopy analysis method: a new analytic method for nonlinear problems. *Applied Mathematics and Mechanics*, *19*, 957-962.

[27] Liao, S. (2004). On the homotopy analysis method for nonlinear problems. *Applied mathematics and computation*, *147*(2), 499-513.

[28] Alkan, A. (2022). Improving homotopy analysis method with an optimal parameter for time-fractional Burgers equation. *Karamanoğlu Mehmetbey Üniversitesi Mühendislik ve Doğa Bilimleri Dergisi*, *4*(2), 117-134.

[29] Arikoglu, A., & Ozkol, I. (2007). Solution of fractional differential equations by using differential transform method. *Chaos, Solitons & Fractals*, *34*(5), 1473-1481.

[30] Merdan, M., Anaç, H., BEKİRYAZICI, Z., & Kesemen, T. (2019). Solving of Some Random Partial Differential Equations by Using Differential Transformation Method and Laplace-Padé Method. *Gümüshane Üniversitesi Fen Bilimleri Enstitüsü Dergisi*, *9*(1).

[31] He, J. H. (1998). Approximate analytical solution for seepage flow with fractional derivatives in porous media. *Computer Methods in Applied Mechanics and Engineering*, *167*(1-2), 57-68.

[32] He, J. H. (1999). Homotopy perturbation technique. *Computer methods in applied mechanics and engineering*, *178*(3-4), 257-262.

[33] He, J. H. (2003). Homotopy perturbation method: a new nonlinear analytical technique. *Applied and Mathematics Computation*, *135*(1), 73-79.

[34] Alquran, M., Al-Khaled, K., & Chattopadhyay, J. (2015). Analytical solutions of fractional population diffusion model: residual power series. *Nonlinear Stud*, *22*(1), 31-39.

[35] Kurt, A., Rezazadeh, H., Senol, M., Neirameh, A., Tasbozan, O., Eslami, M., & Mirzazadeh, M. (2019). Two effective approaches for solving fractional generalized Hirota-Satsuma coupled KdV system arising in interaction of long waves. *Journal of Ocean Engineering and Science*, *4*(1), 24-32.

[36] Şenol, M., Iyiola, O. S., Daei Kasmaei, H., & Akinyemi, L. (2019). Efficient analytical techniques for solving time-fractional nonlinear coupled Jaulent–Miodek system with energy-dependent Schrödinger potential. *Advances in Difference Equations*, *2019*(1), 1-21.

[37] Khuri, S. A. (2001). A Laplace decomposition algorithm applied to a class of nonlinear differential equations. *Journal of applied mathematics, 1,* 141-155.

[38] Akinyemi L (2019) q-Homotopy analysis method for solving the seventh-order time-fractional Lax's Korteweg–de Vries and Sawada–Kotera equations. Comput Appl Math 38(4):1–22.

[39] Akinyemi L, Iyiola OS, Akpan U (2020) Iterative methods for solving fourth- and sixth order time-fractional
Cahn–Hillard equation. Math Methods Appl Sci 43(7):4050–4074.

[40] El-Tawil, M. A., & Huseen, S. N. (2012). The q-homotopy analysis method (q-HAM). *Int. J. Appl. Math. Mech*, *8*(15), 51-75.

[41] El-Tawil, M. A., & Huseen, S. N. (2013). On convergence of the q-homotopy analysis method. *Int. J. Contemp. Math. Sci*, *8*(10), 481-497.

[42] Iyiola, O. S., Soh, M. E., & Enyi, C. D. (2013). Generalised homotopy analysis method (q-HAM) for solving foam drainage equation of time fractional type. *Mathematics in Engineering, Science & Aerospace (MESA)*, *4*(4).

[43] Iyiola, O. S. (2015). On the solutions of non-linear time-fractional gas dynamic equations: an analytical approach. *Int. J. Pure Appl. Math*, *98*(4), 491-502.

[44] Iyiola, O. S. (2016). Exact and approximate solutions of fractional diffusion equations with fractional reaction terms. *Progress in Fractional Differentiation and Applications*, *2*(1), 19-30.

[45] Akinyemi, L. (2020). A fractional analysis of Noyes–Field model for the nonlinear Belousov–Zhabotinsky reaction. *Computational and Applied Mathematics*, *39*(3), 175.

[46] Anaç, H. (2022). Conformable Fractional Elzaki Decomposition Method of Conformable Fractional Space-Time Fractional Telegraph Equations. *Ikonion Journal of Mathematics*, *4*(2), 42-55.

[47] Kartal, A., Anaç, H., Olgun, A. (2023). Numerical Solution of Conformable Time Fractional Generalized Burgers Equation with Proportional Delay by New Methods. *Karadeniz Fen Bilimleri Dergisi*, *13*(2), 310-335.

[48] Erol, A. S., Anaç, H., Olgun, A. (2023). Numerical Solutions of Conformable Time-Fractional Swift-Hohenberg Equation with Proportional Delay by the Novel Methods. *Karamanoğlu Mehmetbey Üniversitesi Mühendislik ve Doğa Bilimleri Dergisi*, *5*(1), 1-24.

[49] Khalil, R., Al Horani, M., Yousef, A., Sababheh, M. 2014. A new definition of fractional derivative. Journal of computational and applied mathematics, 264, 65-70.

[50] Abdeljawad, T. 2015. On conformable fractional calculus. Journal of computational and Applied Mathematics, 279, 57-66.

[51] Ala, V., Demirbilek, U., Mamedov, K. R. 2020. An application of improved Bernoulli sub-equation function method to the nonlinear conformable time-fractional SRLW equation. AIMS Mathematics, 5(4), 3751-3761.

[52] Gözütok, U., Çoban, H., Sağıroğlu, Y. 2019. Frenet frame with respect to conformable derivative. Filomat, 33(6), 1541-1550.